AUI Research Journal

Design of Hardware in the Loop System for Autonomous Ship Carrying Point Scan Sensor (Laser Measurement System)

Hany M. Arnaoot* Gamal Abbas Zaghloul†

Abstract:

*The main objective of the current work is to provide a method through which different control approaches and arrangement applied to autonomous ships carrying a sensor can be investigated and tested. To achieve this a hardware in the loop system was created. This system includes two models (ship model and sensor model). In the current work a sensor simulation algorithm was created and linked to Nomoto ship mathematical model. A **L**inear **Q**uadratic **R**egulator is designed to control simulated ship model.*

The proposed system was applied by a vb.net program to be as close as possible to industrial standard. The program was written as part of the research- to apply suggested simulation algorithm, ship control approach, suggested sensor evaluation and Hardware-in-the-loop system (input and output data through serial port).

The simulation algorithm was verified by in field sea trials on a 11m long yacht with two 250hp outboard engines. the sensor used is sick 218 laser measurement system as a sensor.

Results show that the IMU sensor error has a great effect on the Laser Measurement system processed data and hence environment detection quality.

roll and pitch motion could decrease sensor efficiency dramatically

* Lecturer, Mechatronics Engineering Dept., Alexandria Higher Institute of Engineering & Technology (AIET), Hanyarnaoot@yahoo.com

† Lecturer, Mechanical Power Engineering Dept., Faculty of Engineering, Port Said University.

Keywords: Simulation, Nomoto ship model, LQR, Point scan sensor, Hardware-in-the-loop

1. Introduction:

Over the past few years, autonomous vehicle number and application increase rapidly. It is not limited to a specific field or application. Air Unmanned aerial vehicles (UAVs) have been widely used in various areas ranging from military to entertainment applications. because of reliable control and rapid movement. Recently, these vehicles have been used for searching dangerous or unexpected environments (SungTae Moon, 2015) . At sea there are several applications like autonomous underwater vehicles marine geoscience (Russell B. Wynn, 2014), autonomous unmanned merchant vessel (Hans-Christoph BURMEISTER, 2014). This advance in applications require advance in design, The simulation tools are the foundation for the design of robot systems(Claudio Urrea, 2016). Operator visual monitoring and manual control may be inadequate in complex, cluttered transit environments. Therefore, on-board automatic obstacle avoidance systems may be needed to safely support multiple vessel operations in cluttered complex transit environments(Glenn A. Osga, 2015). The success of the mobile robot navigation control depends mostly on the accuracy of absolute measurements of its position (Anish Pandey, 2014).

Research that involves the use of autonomous vehicle has been divided into three phases: (Dula Nad, 2015)

1- Simulations

2- Navigation guidance and control experiments

3- Create Application scenarios.

Range sensors (such as laser, sonar, radar and stereo vision), are used extensively in the field of robotics for constructing global terrain maps for object avoidance (James Underwood, 2006) (A. Nuchter, 2007).

Along with the increasing use of **L**aser **M**easurement **S**ystems **LMS**, comes the need for a stable and accurate simulation system(Deschaud, 2012).Laser Measurement System is an examples of point scan sensors (standards, 2013).

The proposed algorithm in the current paper meant to predict Point Scan Sensor output data mounted on a moving ship detecting moving objects in different situation.

It could be used when the sensor scan rate is high compared to its extrinsic motion (i.e. motion distortion within the scans can be neglected) or when the sensor scan rate is compared to its extrinsic motion (F. Pomerleau, 2013).

the sensor carrying ship as well as the objects dynamic data (X,Y, Roll and Yaw) are calculated using Nomoto model(Son 1982, Tristan Perez, 2008).

The model presented by Nomoto does not include pitch angle estimation, so pitch angle is not included in calculations. However, current research methodology includes formula for the effect of pitch angle if available. The suggested algorithm has been deployed using a Visual Basic2010 program written for this purpose.

3D calculation requires large computer resources and leads to delay(Gryaznov 2014).It is preferred to avoid using 3D calculation whenever it is possible. The suggested algorithm is meant to simulate point-scanning systems not line scanning systems(standards, 2013). Laser Measurement system sensors has been simulated using modern computer graphics hardware making heavy use of vertex and fragment shaders (Peinecke, 2008).

2. Simulated Vessel characteristics

The ship model used for simulation is the famous four degrees of freedom model which was first introduced by (Mogens Blanke 1997) ***R***oll ***P***lanar ***M***otion ***M***echanism ***(RPMM)*** facility at the Danish Maritime Institute .

The main characteristics of the simulated vessel in the current work in typical operational condition are found in Table 1:

LOA	(length Overall)	175.0	[m]
B	(Beam)	25.0	[m]
T	(Draft)	4.6	[m]
D	(Displacement)	22,200	[ton]
V	(Speed)	20	[kn]

Table 1 simulated vessel characteristics in typical operational condition

Simulated Vessel state space model

Recalling that the x vector of the Nomoto Vessel state space model is defined as (Son 1982) :

$$x = \begin{bmatrix} \mathbf{u} & \mathbf{surge\ velocity} \\ \mathbf{v} & \mathbf{sway\ velocity} \\ \mathbf{r} & \mathbf{yaw\ velocity} \\ \mathbf{x} & \mathbf{position\ in\ x-axis} \\ \mathbf{y} & \mathbf{position\ in\ y-axis} \\ \mathbf{psi} & \mathbf{yaw\ angle} \\ \mathbf{p} & \mathbf{roll\ velocity} \\ \mathbf{phi} & \mathbf{roll\ angle} \\ \mathbf{delta} & \mathbf{actual\ rudder\ angle} \\ \mathbf{n} & \mathbf{actual\ shaft\ velocity} \end{bmatrix}$$

While the input matrix is:

$$\boldsymbol{u_i} = \begin{bmatrix} \boldsymbol{delta\_c} & \boldsymbol{commanded\ rudder\ angle} \\ \boldsymbol{n\_c} & \boldsymbol{commanded\ shaft\ velocity} \end{bmatrix}$$

The model can be written in state space form as(Son 1982, Pradeep Mishra, 2015, Blanke, 2002).

In order to apply LQR linearized model is required, the model parameter is obtained from (Blanke, 2002) , the linearization is done by decoupling the surge equation from the other equations. Thus, a service speed $\bar{u}$ is considered. The approximated value of $\bar{u}$ is calculated as:

$$\approx \frac{\bar{u}-U_{norm}}{U_{norm}} \qquad \textbf{Equation 1}$$

The state vector is reduced to $z = [v\ r\ p\ \varphi\ \psi]$ where:

v	.....	***sway velocity***	*(m/s)*
r	.....	***yaw velocity***	*(rad/s)*
p	.....	***roll velocity***	*(rad/s)*
φ	.....	***roll angle***	*(rad)*
ψ	.....	***yaw angle***	*(rad)*

The linearized model is:

$$A = \begin{bmatrix} \acute{Y}_v & \acute{Y}_p + \acute{Y}_{pu}\,\bar{\acute{u}}_a & \acute{Y}_r + \acute{m}\bar{\acute{u}} & \acute{Y}_\emptyset & 0 \\ \acute{Y}_v & \acute{K}_p + \acute{K}_{pu}\,\bar{\acute{u}}_a & \acute{K}_r + \acute{m}\,\acute{z}_G\bar{\acute{u}} & -(\rho g \acute{\nabla} GM) & 0 \\ \acute{Y}_v & \acute{N}_p + \acute{N}_{pu}\,\bar{\acute{u}}_a & \acute{N}_v + \acute{m}\,\acute{z}_G\bar{\acute{u}} & \acute{N}_\emptyset & 0 \\ 0 & 1 & 0 & 0 & 0 \\ 0 & 0 & 1 & 0 & 0 \end{bmatrix} \qquad \textbf{Equation 2}$$

$$: \begin{bmatrix} \acute{Y}_\delta \\ \acute{K}_\delta \\ \acute{N}_\delta \\ 0 \\ 0 \end{bmatrix} \qquad \textbf{Equation 3}$$

The numerical model is:

The input matrix:

$$A = \begin{bmatrix} -0.07250 & 0.00000 & 0.00620 & 0.00380 & 0.00000 \\ 0.002500 & -0.0003 & -0.0199 & -379.9796 & 0.00000 \\ -0.0300 & -0.0006 & -0.0489 & -0.0018 & 0.00000 \\ 0.00000 & 1.00000 & 0.00000 & 0.00000 & 0.00000 \\ 0.00000 & 0.00000 & 0.00000 & 0.00000 & 0.00000 \end{bmatrix}$$ ation 4

$$\begin{bmatrix} 0.0248 \\ -0.0007 \\ -0.0129 \\ 0.000 \\ 0.000 \end{bmatrix}$$ ation 5

Ship controller Design

In the present work two controller

are suggested, the first is the ***P***roportional ***D***erivative PD Controller, the Linear Quadratic Regulator LQR and the Linear Quadratic Gaussian LQG.

The suggested controllers are used to …….

LQR controller Design

Recalling that The optimal control law is obtained as:

$$- k x$$ ation 6

Where k is the feedback gain matrix, it is defined by:

$$R^{-1}BTS$$ ation 7

Where S is the solution of algebraic Matrix Riccati Equation (MRE)

$$+ A^{T}S - SBR^{-1}B^{T} S+ Q = 0$$ ation 8

The feedback gain matrix for A and B matrix in Equation 4 and Equation 5 was calculated to be

$$k = [\, 2.4448 \quad -0.0786 \quad -12.6437 \quad 0.4462 \quad -1.0000]$$

$$s = 1.0e^{05}\begin{bmatrix} 0.0001 & -0.00 & -0.0010 & -0.00 & -0.0002 \\ -0.0000 & 0.0166 & 0.0000 & 0.0000 & 0.0000 \\ -0.0010 & 0.0000 & 0.0087 & 0.0003 & 0.0012 \\ -0.0000 & 0.0000 & 0.0003 & 6.3045 & 0.0000 \\ -0.0002 & 0.0000 & 0.0012 & 0.0000 & 0.0002 \end{bmatrix}$$

The Eigen values

$$e = 1.0e^{05}\begin{bmatrix} -0.0002 + 19.4931i \\ -0.0002 - 19.4931i \\ -0.1008 + 0.0393i \\ -0.1008 - 0.0393i \\ -0.1435 + 0.0000i \end{bmatrix}$$

The sensor simulation Model

Before proceeding with mathematical modeling two terms must be well defined the first term is the object(s) corners lines, which are the group of lines forming the object shape for the case of rectangle, there are four points and hence four corner lines. These lines are extruded to form a three-dimensional object in this case a parallelepiped.

The following Figure 1 shows a wedge shaped target two-dimensional and three-dimensional sketch.

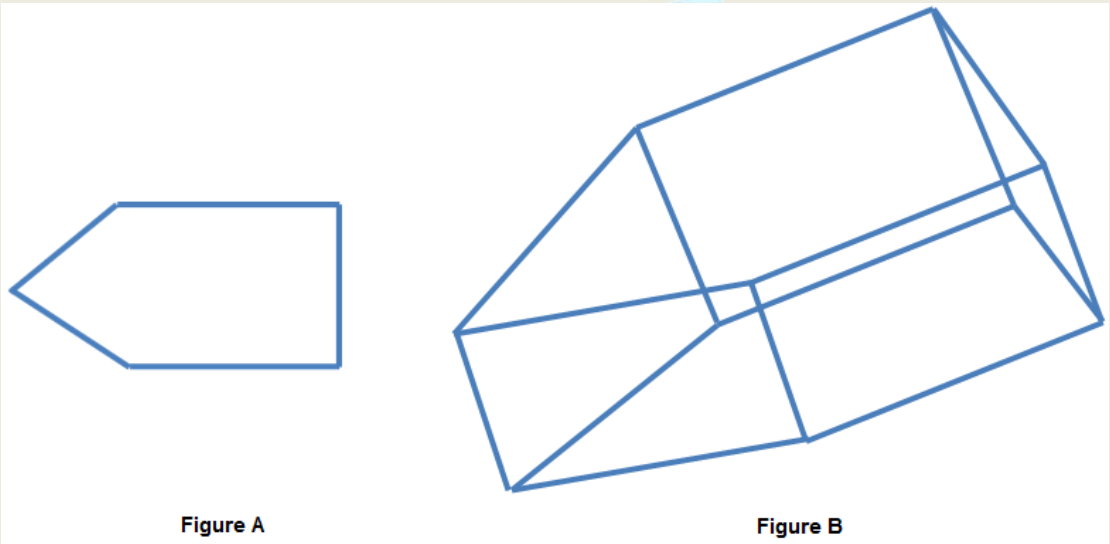

Figure A Figure B

Figure 1 Figure A 2D sketch of a shape , Figure B 3D extrusion of shape A.

The Second term is the scanning line, which is the line beginning at current sensor carrying vehicle position and ends at sensor maximum range at current scan line angle).

The proposed simulation model in this paper was inspired by mathematical model developed by (Gamal Zaghloul, 2015)

The algorithm could be summarized as follows:

1. Calculate the sensor-carrying vehicle and other object position and orientation in space using the appropriate mathematical model to obtain sensor X, Y, Z-axis position and orientation (in the present work Nomoto mathematical model is used).
2. Calculate Scan Line start co-ordinates in X, Y, Z-axis starting from sensor carrying vehicle position and orientation and current sensor scan angle using the following two formulas.
3. Calculate Scan Line end co-ordinates using the spherical co-ordinates, and transfer it back to Cartesian co-ordinates see Figure 1 and Figure 3 Figure **3 Relation between scan line start, ends, and vehicle position** .

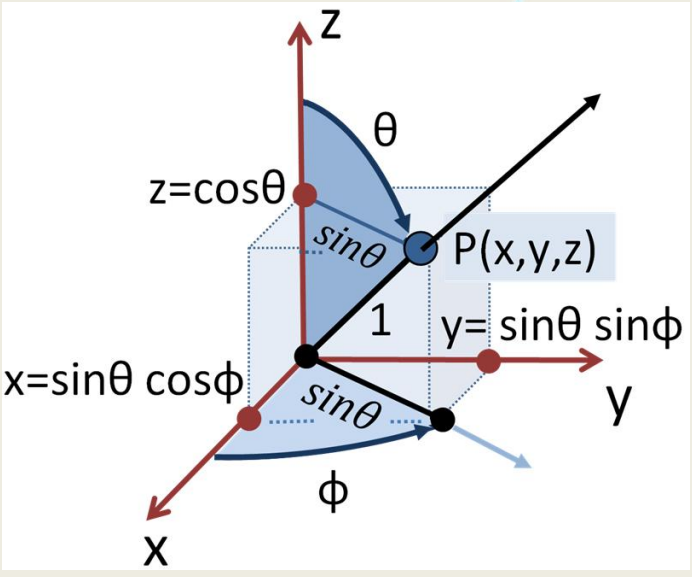

Figure 2 Relation between Cartesian and Polar co-ordinates

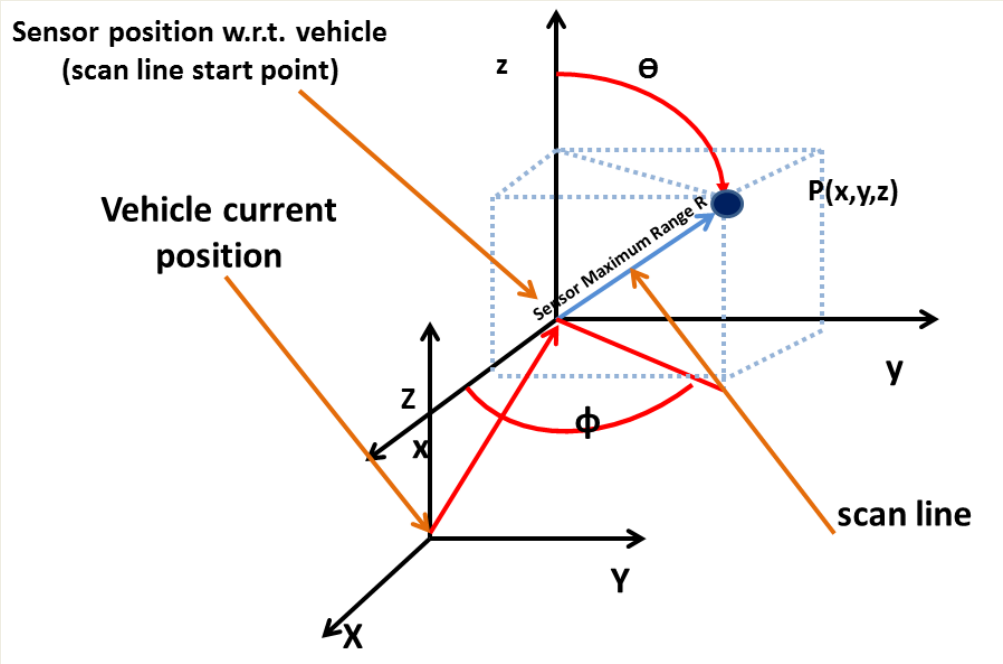

Figure 3 Relation between scan line start, ends, and vehicle position

4. Calculate the co-ordinates of the points forming the simulated object(s). These point co-ordinates change in two cases the first is when the object(s) position change(s); the second is when the object(s) orientation change(s).
5. Calculate the rotation matrix for each object according to it's calculated (pitch, roll, yaw) angles using the formula.
6. Calculate new co-ordinates of points forming the simulated object(s) using the calculated rotation matrix.
7. Calculate intersection point(s) P(x, y) co-ordinates between every obstacle corner plane and scan line using algorithm in (Ericson, 2005).

Moller's algorithm generalizes and optimizes Badouel's. It is based on the transformation of the triangle and the ray so that the triangle is translated to the origin of the coordinate system and is scaled in order to obtain a unit triangle on yz-plane with the ray aligned with the x-axis(Juan J. Jiménez, 2010) ,see Figure **4**.

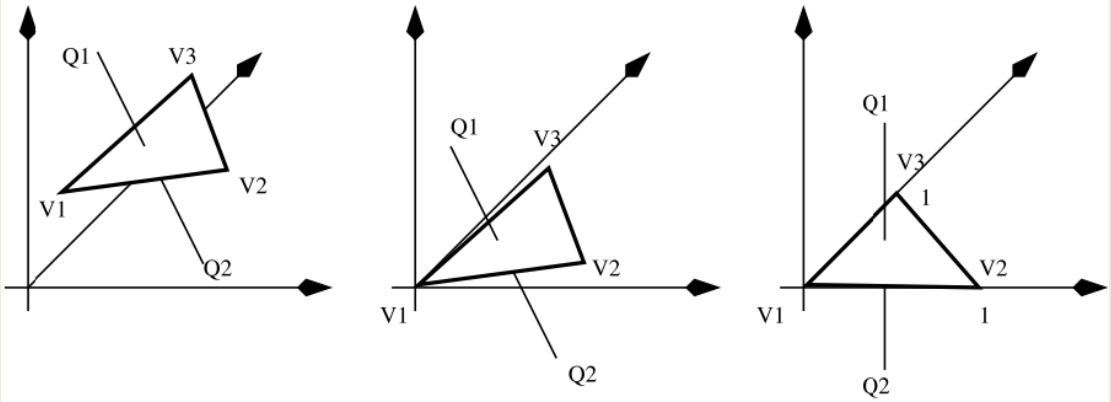

Figure 4 transformation of the triangle and the ray

By using, the barycentric coordinates of a point with regard to a triangle

$$S(u, v) = (1-u-v) \cdot V1 + u \cdot V1 + v \cdot V1$$

The point is defined as belonging to the triangle if it satisfies $u \geq 0$, $v \geq 0$ and $u+ v \leq 1$. If the ray equation is equaled to the point equation, the intersection point is calculated as follows:

$$Q1+t \cdot (Q2- Q1) = (1 - u - v) \cdot V1+ u \cdot V2+ v \cdot V3$$

When this equation is solved, the following result is obtained

8. Remove fake scan matrix results using methods proposed by (Gamal Zaghloul, 2015).
9. Applying previous equations with the scan line and each obstacle corner plane yields a set of points.
10. For each detected point, calculate the distance between intersection point and sensor carrying vehicle current position.
11. The resulting scan time, scan angle and range is the sensor output data.

The developed Simulation software for the research:

In this work, the author introduces a suggested VB.net computer program. The program input is the simulated ship parameters (length, width, maximum rudder angle …), sensor parameters (sensor maximum range, Sensor mounting point height …), simulation initial conditions (initial vehicle position, initial sensor angle…) and simulated objects shape.

Simulated object Shape is defined by a set of lines. Each line is defined by (range, angle). When the object position or course changes during simulation, each line start and end coordinates is recalculated.

The suggested algorithm is applied to a vb.net not a mat lab code (although it is much difficult) to reduce computation loading on the processor. Reducing processing time make it close to industry point of view. Also to create Hardware in the loop for sick LMS 221 sensor (Khalid bin Hasnan and 2012).

The developed program plots the vehicle, the object(S) and the detected point(s) in three dimension to facilitate analyzing and understanding of the results.

The program also plots the vehicle dynamic characteristics change with time (x,y,z position rudder angle, roll angle, roll velocity….).

The program Graphical user interface GUI is shown in **Error! Reference source not found.**Figure B

Figure 5

AUI Research Journal

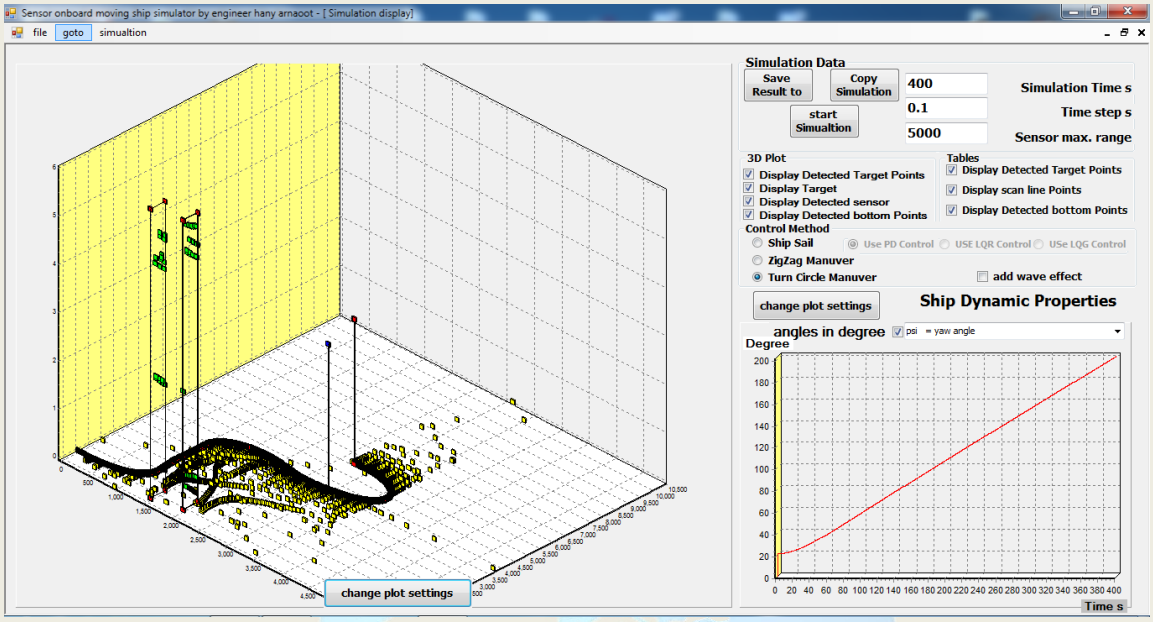

Figure A

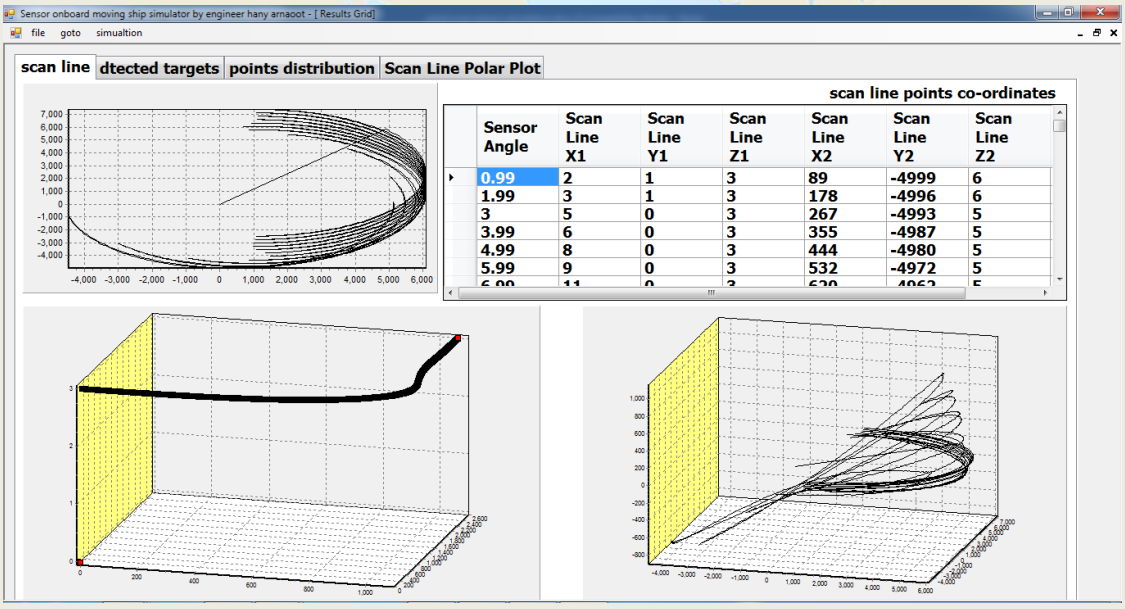

Figure B

Figure 5 Graphical User Interface GUI of the suggested VB.net 2010 computer program.

Sensor Simulation algorithm verification:

In order to evaluate the performance of the suggested Sensor Simulation algorithm, a comparison between a collected simulated sensor data and the actual collected sensor data. This is very difficult because ship simulation model and environmental conditions (wind, current, tide) simulation performance will affect suggested system performance. To focus on Sensor Simulation algorithm verification and simplify the verification process a number of sea trials was carried out.

Ship used for sea trials:

the ship used is an eleven meters long yacht with 3-ton displacement, propulsion system is two 250 horse power outboard engines which makes a total of 400 horse power, See Figure 6. The yacht has achieved a maximum speed of 35 knots in calm sea state

Figure 6 used yacht for sea trials

Sensors used in verification process

There are three main sensors used in the verification process the point scan sensor which is selected as Sick LMS221, the differential Global positioning system device DGPS which is selected as differential GPS Trimble R7 and GPS Receiver, the gyro compass which is selected as gyrotrac and the displacement – rotation measuring device (to determine roll and pitch)

The laser measurement system (Sick LMS221)

The laser measurement system (Sick LMS221)(2006) is mounted on top of the yacht super structures on the middle.an image of the Sick LMS221 is shown in Figure 7.

Figure 7 A close image of the sick LMS221 laser measurement system

The distance value per individual impulse (spot) is evaluated. This means that a distance value is provided every 0.25°, 0.5° or 1°, depending on the selected angular resolution of the sensor. In the current work the simulation as well as sea trials was carried out using 1° resolution. The sensor data is collected through serial port (RS 232) interface to main computer. The spot spacing in cm versus range in m for (0.25°, 0.5° or 1°) angular resolution is shown in Figure 8

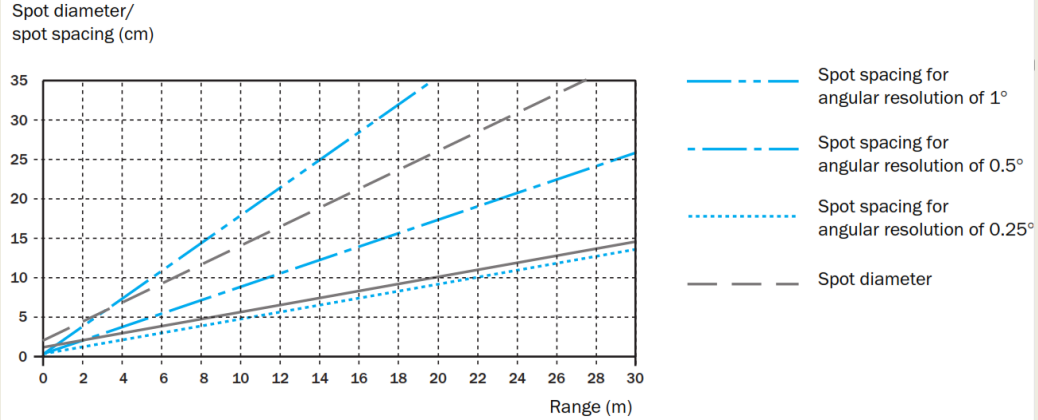

Figure 8 spot spacing in cm versus range in m for (0.25°, 0.5° or 1°) angular resolution

The range of the LMS2xx depends on the reflectivity of the target object and the transmission strength of the LMS221

Some reflectivity values for well-known materials are listed Table 2 as an overview (KODAK standards).

Material	Reflectivity
Cardboard, matt black	10%
Cardboard, grey	20%
Wood (raw pine, dirty)	40%
PVC, grey	50%
Paper, matt white	80%
Aluminum, anodized, black	110% to 150%
Steel, rust-free shiny	120% to 150%
Steel, very shiny	140% to 200%
Reflectors	> 2000%

Table 2 Some reflectivity values for well-known materials

The relation between reflectivity and detection range is found Figure 9

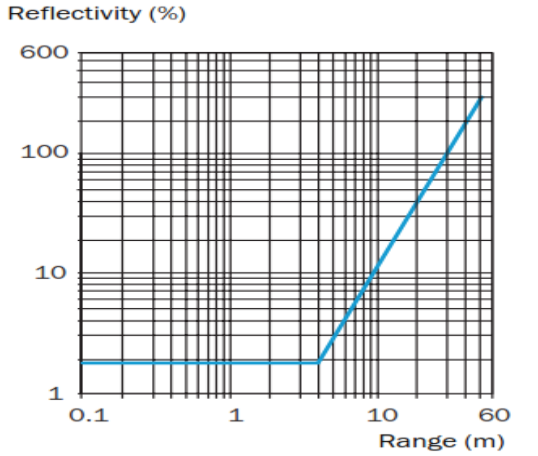

Figure 9 relation between reflectivity and detection range

Gyro compass

The Gyro compass is used to estimate the absolute ship heading (yaw) and hence absolute sensor heading, a Gyrotrac is selected see Figure 10

Figure 10 Gyrotrac magnetic gyro compass

Differential GPS

A differential GPS Trimble R7 GPS and Receiver is used to estimate the absolute ship position (easting and northing), data is collecting through a serial port with Baud rates 9600 bps. The Output format is NMEA-0183. The estimated error is about 0.5 to 1.0 meter

IMU unit

An IMU is used to estimate the ship orientation in space roll, pitch and yaw. The yaw data is obtained from the gyro compass.

Hardware-in-the-loop system

Hardware-in-the-loop or HIL is relatively new technique. It is used to test the design of a controller when performing Model-Based Design in the development and testing of complex real-time embedded systems. For the current case a sensor onboard a ship, the main purpose of the current HIL is to test embedded system controller in various conditions without having to do sea trials.

The HIL sends data to the controller through 4 serial ports as follows:

1- Simulated range data obtained from suggested sensor simulation algorithm organized as (header , range data composed of two bytes per each point , footer and checksum)(2006) . This channel is connected in the socket of Sick LMS221 range measurement sensor.

2- Simulated ship position (easting and northing) obtained from Nomoto model as NMEA-0183 format. This channel is connected in the socket of differential GPS.

3- Simulated ship yaw angle obtained from Nomoto model as NMEA-0183 format. This channel is connected in the socket of differential GPS.

4- Simulated ship pitch and roll obtained from Nomoto model. This channel is connected in the socket of differential GPS.

3. USED SIMULATION METHODOLOGY FIELD VERIFICATION:

Sea conditions affecting ship motion (wave, wind, tide and current) are complicated and very hard to reproduce using math models and it is not the scope of the current work. To verify used simulation methodology the ship sensors data

were recorded (instead of generating them using Nomoto model) and compared to simulated suggested sensor model output.

The following figures is a sample of a field verification process in which the ship change heading from east to north. this heading change causes the ship to roll to the portside causing the laser scanner to hit sea which produce false target points.

In order to facilitate data visualizing the ship position in space is combined with the laser measurement sensor to get a series of points in 3-dimensional space, the data for the field collected sensor data and simulated data is shown in the following figure

4. RESULTS

The simulation field verification was carried out in open sea. Laser Measurement Sensor which is mounted perpendicular to the mast i.e. parallel to sea surface. When the ship rolls or pitch, the sensor points to the sky (preventing detection of targets in range) or to sea surface (producing false data).

In the verification process the sensor scans in open sea detecting sea surface. This because of two reasons, the first is the difficulty of setting up a fixed target in the open sea to be detected by the sensor, the second is that the target shape and material reflectivity may not be the same which will affect the resultant scan data and hence harden the process of evaluating the suggested algorithm.

4.1 RESULTS during 90º course change

The following figures (**Error! Reference source not found.** to figure 13) are field sea trial logged data during turning in a full circle, while **Error! Reference source not found.** and **Error! Reference source not found.** represent the simulated versus the real sensor collected data.

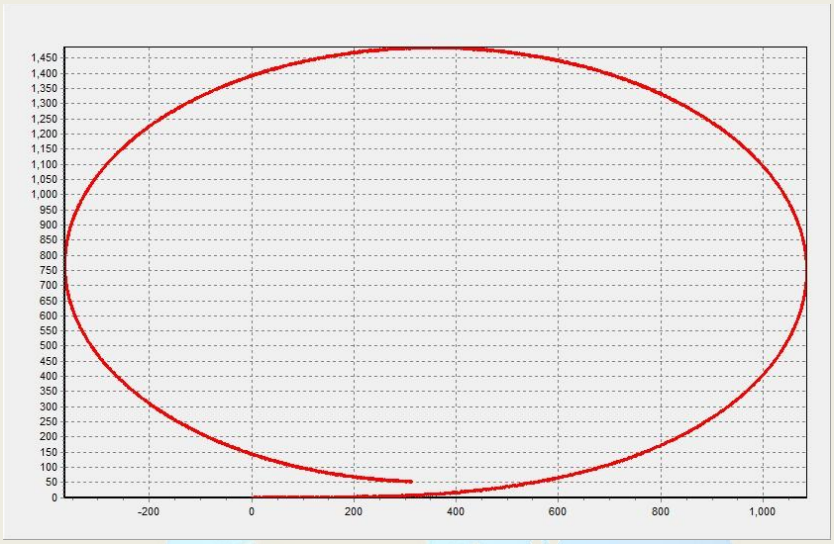

Figure 11 Field sea trial logged data during turning in a full circle (ship course)

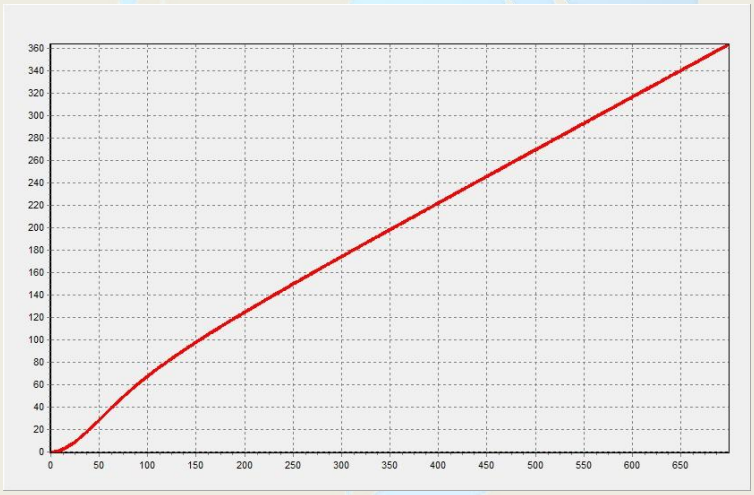

Figure 12 Field sea trial logged data during turning in a full circle (ship yaw angle)

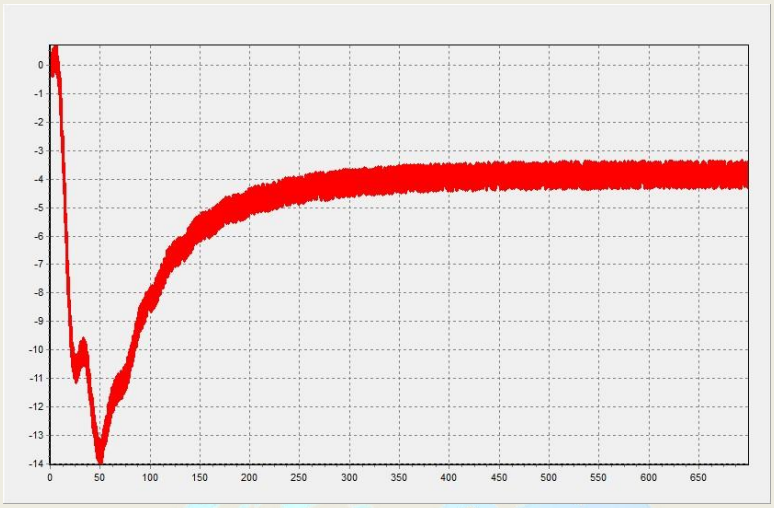

Figure 13 Field sea trial logged data during turning in a full circle (ship roll angle)

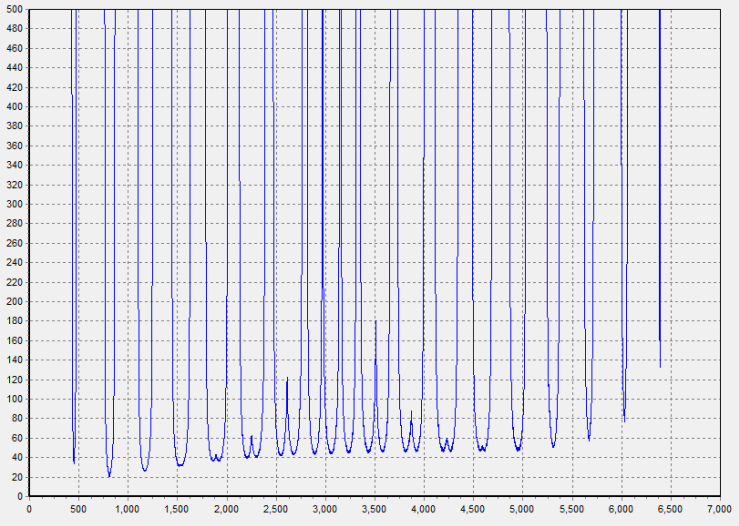

Figure 14 Real range sensor data versus time based on collected Field sea trial logged data during turning in a full circle

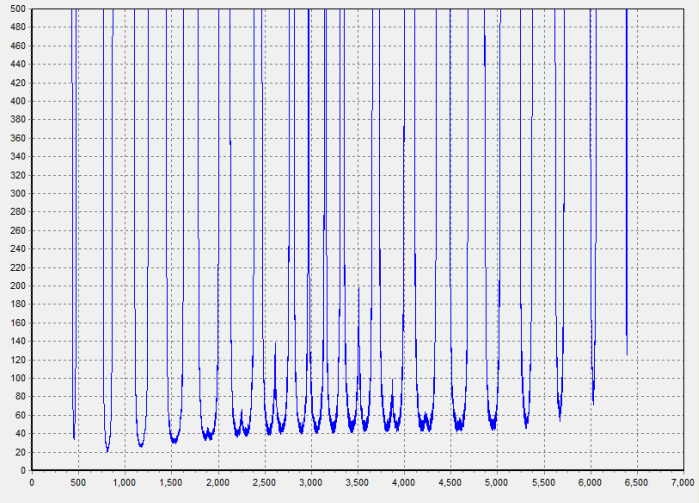

Figure 15 Simulated range sensor data versus time based on collected Field sea trial logged data during turning in a full circle

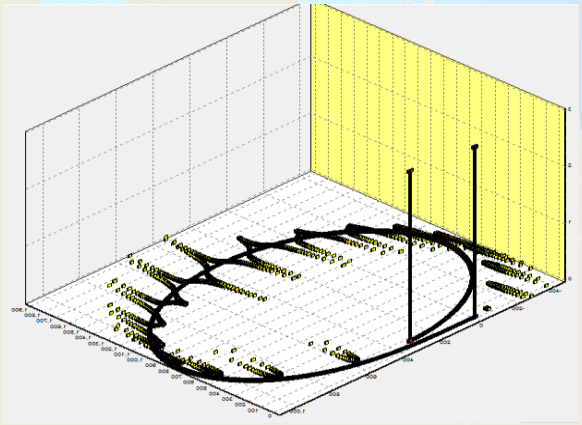

Figure 16 A 3D plot of ship path (bottom black circle) and detected sea surface points (yellow points) during

4.2 RESULTS during 90º course change

The following figures (**Error! Reference source not found.** to) are field sea trial logged data during changing course from 0º to 90º, while **Error! Reference source not found.** and **Error! Reference source not found.** represent the simulated versus the real sensor collected data.

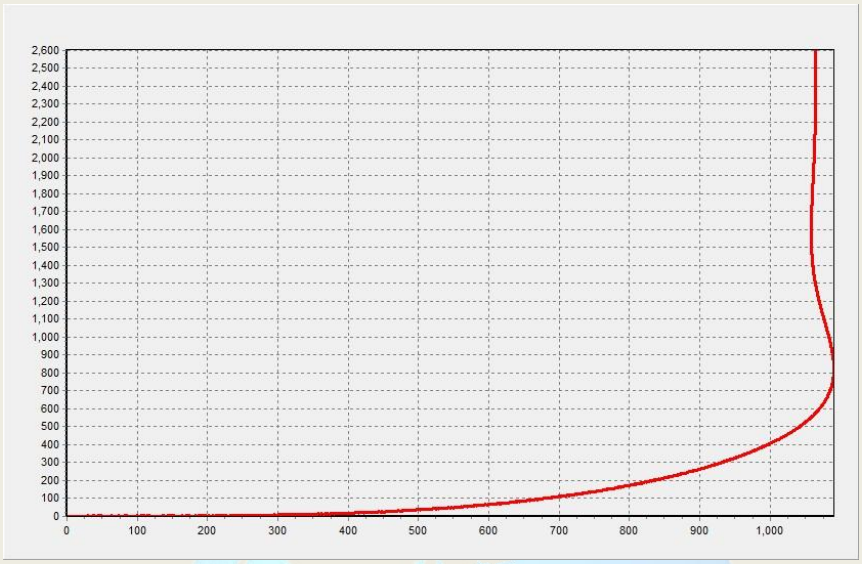

Figure 17 Field sea trial logged data during changing course from 0º to 90º (ship course)

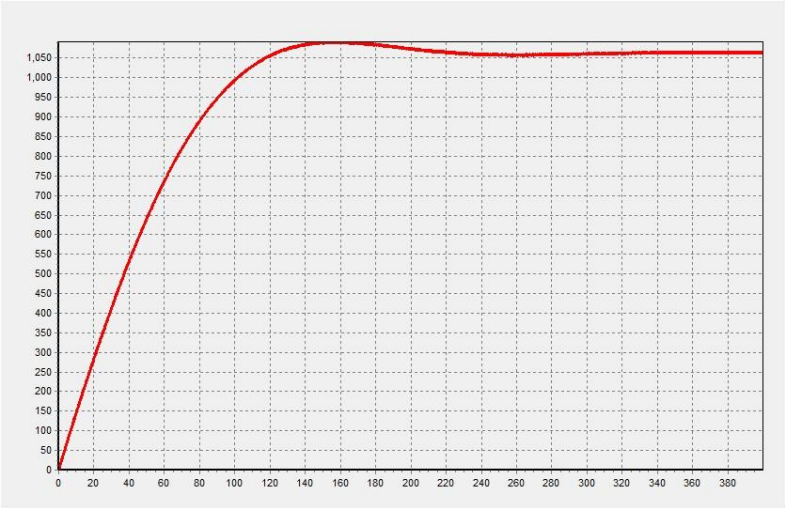

Figure 18 Field sea trial logged data during changing course from 0º to 90º (ship yaw angle)

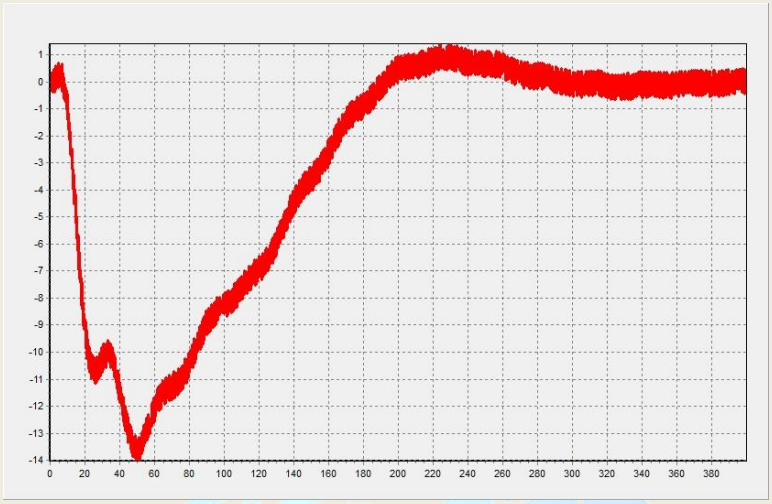

Figure 19 Field sea trial logged data during changing course from 0º to 90º (ship roll angle)

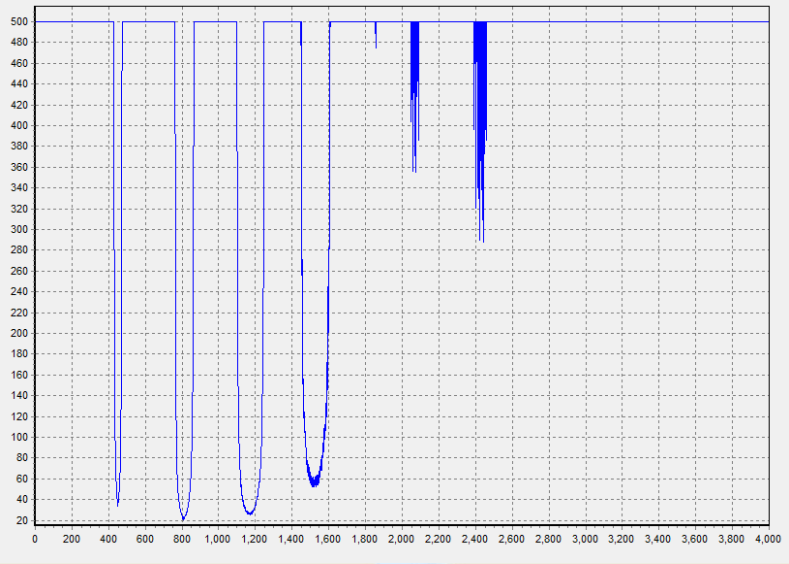

Figure 20 Simulated range sensor data versus time based on collected Field sea trial logged data during changing course from 0º to 90º

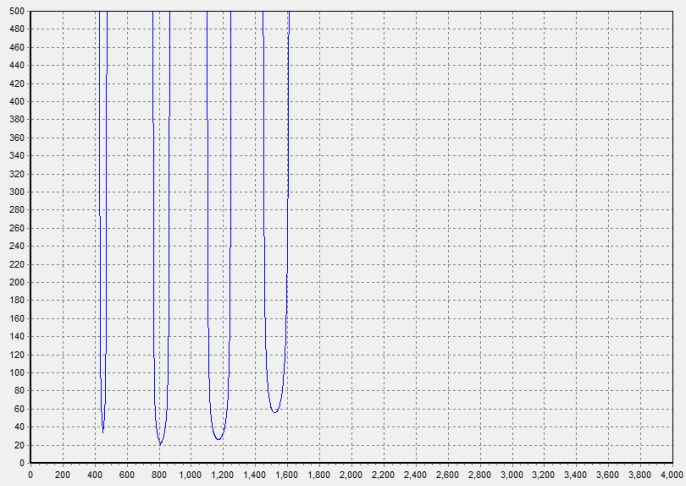

Figure 21 Real range sensor data versus time based on collected Field sea trial logged data during changing course from 0º to 90º

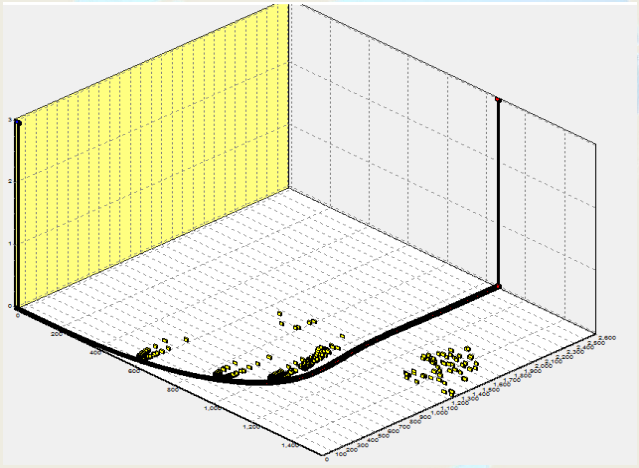

Figure 22 A 3D plot of ship path (bottom black circle) and detected sea surface points (yellow points) during

5. Comment on the results

As seen when comparing Figure 14 with Figure 15 and Figure 20 with Figure 21 the real scan matrix data is relatively uniform. in **Error! Reference source not found.** the simulated scan matrix data is not as uniform as the real.

The lack of uniformity is believed to be due to data sensors error. to verify this theory a random error was injected into to the simulated data. the results showed nonuniformity that increase with injected error margin increase.

6. Conclusion

1. Environment identification sensor are sensitive to position in space sensor specially IMU sensor.
2. The synchronization between position sensors is very important specially when the Environment identification sensor scan speed is comparable to:
   a- Change of ship position or orientation in space
   b- Rate of ship position or orientation in space sensor data output

The Future Work can be summarized as:

Analyzing sensor error and uncertainty and their effect on range error.

7. References

2006. LMS200/211/221/291 Laser Measurement Systems TECHNICAL DESCRIPTION. *In:* WALDKIRCH, S. A. (ed.).

A. NUCHTER, K. L., J. HERTZBERG, AND H. SURMANN 2007. 6D SLAM – Mapping Outdoor Environments. *Journal of Field Robotics,* 24**,** 699–722.

ANISH PANDEY, D. R. P. 2014. MATLAB Simulation for Mobile Robot Navigation with Hurdles in Cluttered Environment Using Minimum Rule Based Fuzzy Logic Controller. *2nd International Conference on Innovations in Automation and Mechatronics Engineering,ICIAME 2014 , elsevier,* 14**,** 7.

BLANKE, T. S. P. E. A. M. 2002. *Mathematical Ship Modeling for Control Applications*.

CLAUDIO URREA, J. K. 2016. Design, simulation and comparison of controllers for a redundant robot. *Case Studies in Mechanical Systems and Signal Processing, elsevier,* 3**,** 13.

DESCHAUD, J. E., PRASSER , D., DIAS, M.F., BROWNING, B., RANDER,P. 2012. Automatic Data Driven Vegetation

Modeling for LIDAR Simulation. *U.S. Army Engineer Research and Development Center, (ERDC) under cooperative agreement "Fundamental Challenges in World and Sensor Modeling for UGV Simulation,* (Number W912HZ-09-2-0023)**,** 7.

DULA NAD, N. M., FILIP MANDI 2015. Navigation, guidance and control of an overactuated marine surface vehicle. *Elsevier,* 40**,** 172–181

ERICSON, C. 2005. *Real-Time Collision Detection,* United States of America, Morgan Kaufmann Publishers is an imprint of Elsevier.

F. POMERLEAU, F. C., R. SIEGWART, AND S. MAGNENAT 2013. Comparing ICP Variants on Real-World Data Sets Open-source library and experimental protocol. *Autonomous Robots,* 34**,** 133–148.

GAMAL ZAGHLOUL, H. A. 2015. Simulation of a Laser Measurement System LMS Sensor Mounted on a Moving Vehicle Detecting Moving Obstacles. *Proceedings of the 16th International Conference on Aerospace Sciences and Aviation Technology,* 1**,** 11.

GLENN A. OSGA, M. R. M. 2015. Human-computer interface studies for semi-autonomous unmanned surface vessels. *Procedia Manufacturing , elsevier,* 3**,** 8.

GRYAZNOV , N. A. L., A., 2014. Computer Vision for Mobile On-Ground Robotics. *25th DAAAM International Symposium on Intelligent Manufacturing and Automation***,** 5.

HANS-CHRISTOPH BURMEISTER, W. B., ØRNULF JAN RØDSETH, THOMAS PORATHE 2014. Autonomous Unmanned Merchant Vessel and its Contribution towards the e-Navigation Implementation: The MUNIN Perspective. *International Journal of e-Navigation and Maritime Economy, elsevier,* 1**,** 13.

JAMES UNDERWOOD, A. H., DR. STEVE SCHEDING 2006. Calibration of Range Sensor Pose on Mobile Platforms. *IEEE/RSJ International Conference on Intelligent Robots and Systems*, 6.

JUAN J. JIMENEZ, R. J. S., FRANCISCO R. FEITO 2010. A robust segment/triangle intersection algorithm for interference tests. Efficiency study. *Elsevier, Computational Geometry* 43, 474–492.

KHALID BIN HASNAN, L. B. S. A. T. H. & 2012. A Hardware-In-the-Loop Simulation and Test for Unmanned Ground Vehicle on Indoor Environment *2012 International Workshop on Information and Electronics Engineering (IWIEE)* 29, 5.

MOGENS BLANKE , A. G. J. 1997. Dynamic Properties of Container Vessel with Low Metacentric Height. *Technical Report doc. No. R-1997-4173.* Denmark: Aalborg University.

PEINECKE, N., LUEKEN, T., KORN, B.R., 2008. LIDAR simulation using graphics hardware acceleration. *Digital Avionics Systems Conference, 2008. DASC 2008. IEEE/AIAA 27th,* 4, 8.

PRADEEP MISHRA, S. K. P., SWARUP DAS 2015. Ships Steering Autopilot Design by Nomoto Model. *International Journal on Mechanical Engineering and Robotics (IJMER)* 3, 6.

RUSSELL B. WYNN, V. A. I. H., TIMOTHY P. LE BAS 2014. Autonomous Underwater Vehicles (AUVs): Their past, present and future contributions to the advancement of marine geoscience, elsevier. *elsevier,* Marine Geology 352, 18.

SON , K. H. A. N. 1982. On the Coupled Motion of Steering and Rolling of a High Speed Container Ship, Naval Architect of Ocean Engineering. *J.S.N.A.,* 150, 10.

STANDARDS, N. C. F. G. I. 2013. *Light Detection and Ranging LIDAR Sensor Model Supporting Precise Geopositioning,* USA, National center for geospatial intelligence standards.

SUNGTAE MOON, W. E., HYUNCHUL GONG 2015. Development of Large-Scale 3D Map Generation System for Indoor Autonomous Navigation Flight – work in progress *"APISAT2014", 2014 Asia-Pacific International Symposium on Aerospace Technology, elsevier,* 99**,** 5.

TRISTAN PEREZ, T. L. 2008. guidance, navigation and control Matlab toolbox,. *guidance, navigation and control Matlab toolbox,.*